ISTITUTO NAZIONALE DI FISICA NUCLEARE

Sezione di Torino

INFN/TC-92/11
13 Aprile 1992

C. Manfredotti, A. Zanini, M. Boero, C. Ongaro, F. Fizzotti:

PHENOMENOLOGICAL ANALYSIS OF THE $Li(n,\alpha)T$ SCATTERING IN PLASMA PRODUCED NEUTRONS

Servizio Documentazione
dei Laboratori Nazionali di Frascati

INFN – Istituto Nazionale di Fisica Nucleare
Sezione di Torino

INFN/TC–92/11
13 Aprile 1992

PHENOMENOLOGICAL ANALYSIS OF THE $Li(n,\alpha)T$ SCATTERING IN PLASMA PRODUCED NEUTRONS

C. Manfredotti, A. Zanini *, M. Boero, C. Ongaro and F. Fizzotti

Experimental Physics Dept., University of Torino and
*Istituto Nazionale di Fisica Nucleare - sezione di Torino

Abstract

In the present work is discussed and analyzed the nuclear reaction

$$^{6}_{3}Li + n \rightarrow \alpha + T$$

which should take place in the detection process of neutrons [1,2] coming out from a deuterium–deuterium (D–D) and deuterium–tritium (D–T) plasma. The purpose is to evaluate the error on the detected neutron energy from the knowledge of the errors on emission angle and energy of the α particles produced in the above quoted process.

Calculations have been performed by means of canonical energy–momentum conservation laws in the laboratory frame and the results are used to predict the energy and angle resolution requested by a hypothetical α particles detector in order to obtain a good plasma diagnostics.

1. Introduction

The problem of neutron diagnostics [3] as a method to gain informations on the plasma ion temperature has already been discussed [5,9]. In what follows the nuclear reaction involved in the detection process is analyzed and discussed.

Neutrons are supposed to be produced in a deuterium–deuterium (D–D) and deuterium–tritium (D–T) plasma, with typical 2.45 MeV and 14.02 MeV fusion energies and detected in regions far from the plasma chamber. The energy range of the outcoming neutrons has been chosen as a continuous interval from 0 up to 14.02 MeV according to the Monte Carlo MCNP simulations (details have been given elsewhere in Refs. 4 and 5).

It has been indicated [5] that the neutron peak width w is related to the ion temperature T_i by the relationships

$$w = 177 \cdot \sqrt{T_i\ (KeV)} \qquad D-T$$

$$w = \ 82 \cdot \sqrt{T_i\ (KeV)} \qquad D-D$$

and, consequently, if one wants to measure a plasma temperature of $T_i = 10\ KeV$ with an uncertainty of 1 KeV, the corresponding neutron peaks will have widths of 560 and 260 KeV respectively, and they should be measured or reconstructed with an uncertainty of at least 28 KeV and 13 KeV respectively. Only a spectrometer with extremely high performances could achieve could achieve the required accuracy. The design parameters of such spectrometers must be defined theoretically. Roughly speaking, one can obtain an indication of the needed efficiency by assuming that a total of 2000 counts are to be present in the peak and that the energy resolution must be better than 100 KeV and 50 KeV for the two reactions respectively [5].

The purpose of the present work is to analyze the $Li(n,\alpha)T$ scattering with two particles in the initial state and two particles in the final one. This is the nuclear reaction occurring in a Lithium target [10] absorbing the neutrons coming from the plasma and emitting α particles whose scattering angle and energy are measured. The accuracy of this measure is crucial to evaluate the energy of the incoming neutron, which is a skilful piece of information in plasma diagnostics [5].

2. Analysis of the $Li(n,\alpha)T$ scattering

The problem of plasma diagnostics by detection of emitted neutrons in a JET–like apparatus [6] has already been discussed in a previous paper [4]. The nuclear reaction which has been planned to adopt as neutron detection technique is the absorption of n in a Li target. The products of this reaction are, as it is well known [2], tritium T and α particles ${}^4_2He$. The scattering

$${}^6_3Li + {}^1_0n \ \rightarrow \ {}^4_2He + {}^3_1H + Q \tag{1}$$

is a slow absorption process where the released energy is $Q = 4.78\ MeV$ and it can be assumed exactly known [2,7].

Relativistic calculations are in principle needed to take into account the mass–to–energy conversion represented by $Q > 0$ in the final products, but non–relativistic simplifications can be adopted as shown below. The four–momentum $p_\mu = (E, -c\mathbf{p})$ conservation rule, i.e.

$$p_\mu p^\mu = m^2c^4 \quad \Rightarrow \quad E^2 = \mathbf{p}^2c^2 + m^2c^4 \tag{2}$$

is imposed in the laboratory frame and all the results will be referred to this choice.

In order to simplify the labels a numerical index j has been set up,

$$j \equiv [1 = n\ ,\quad 2 = Li\ ,\quad 3 = T\ ,\quad 4 = \alpha]$$

to identify each particle involved in the process. In addition, m_j is intended as the $j-th$ particle rest mass and therefore

$$\gamma_j = \frac{1}{\sqrt{1-\frac{v_j^2}{c^2}}} \qquad M_j = m_j c^2$$

$$E_j = \gamma_j m_j c^2 \qquad \mathbf{P}_j = \gamma_j m_j \mathbf{v}_j$$

where c is the light speed and $\mathbf{v}_j$ the laboratory frame velocity. With these notations, the energy–momentum conservation can be written as

$$p_{\mu,j} p_j^{\mu} = E_j^2 - \mathbf{P}_j^2 c^2 = M_j^2 \quad . \tag{3}$$

The laboratory frame is the rest frame of the Li target nucleus. This means that the complete set of equations (3) takes the form

$$E_1 + M_2 = E_3 + E_4 \tag{4a}$$

$$P_1 = P_3 \cos\theta_3 + P_4 \cos\theta_4 \tag{4b}$$

$$P_3 \sin\theta_3 = P_4 \sin\theta_4 \tag{4c}$$

where the angles are measured according to Fig. 1 and $|\mathbf{P}_j| = P_j$. Squaring and summing up Eq. (4b) and (4c) it is possible to obtain the equation

$$P_1^2 + P_4^2 - 2P_1 P_4 \cos\theta_4 = P_3^2 \tag{5}$$

and recover the non–relativistic approximation as the energies involved in the nuclear reaction are sufficiently small, i.e.

$$\gamma_j \simeq 1 + \frac{1}{2}\frac{v_j^2}{c^2}$$

As a consequence, energy and momentum can be expanded up to the second order in the velocity

$$E_j \simeq m_j c^2 \cdot \left(1 + \frac{1}{2}\frac{v_j^2}{c}\right) = M_j + T_j \tag{6}$$

$$\mathbf{P}_j \simeq m_j \mathbf{v}_j \cdot \left(1 + \frac{1}{2}\frac{v_j^2}{c}\right) \simeq m_j \mathbf{v}_j \quad . \tag{7}$$

where T_j is the kinetic energy of the $j-$th particle, related to the squared momentum by the obvious relation

$$\mathbf{P}_j^2 c^2 = 2M_j T_j \tag{8}$$

rather similar to the classical formula. Following the standard procedure, it is possible to define the released energy of the slow absorption reaction, $Q = M_1 + M_2 - (M_3 + M_4)$ so that the complete set of equations governing the neutron scattering takes the form

$$T_1 + Q = T_3 + T_4 \tag{9a}$$

$$P_1^2 c^2 + P_4^2 c^2 - 2c^2 P_1 P_4 \cos\theta_4 = P_3^2 c^2 \tag{9b}$$

Eq. (9a) can then be used to estimate the errors ΔT_1 which affects the neutron energy measured value if the errors on the tritium energy, ΔT_3, and on the α particle ΔT_4 are independently known,

$$\Delta T_1 = \sqrt{\sum_{j=3}^{4} \left(\frac{\partial T_1}{\partial T_j}\right)^2 (\Delta T_j)^2} = \sqrt{(\Delta T_3)^2 + (\Delta T_4)^2} \quad . \tag{10}$$

However, the detection process is oriented to the measurements of energy and emission angle of the α particles only, while no attention is payed to the tritium [1,8] and so the Eq. (10) has no practical application in error estimations. Then it is convenient to refer each dependence of the function T_1 to ${}^4_2He$ variables, i.e. scattering energy and angle. This can be obtained by direct substitution of (9a) into (9b) and using the afore quoted relation (8) between kinetic energy and momentum to eliminate the dependences on momenta,

$$(M_1 - M_3)T_1 + (M_3 + M_4)T_4 - M_3 Q = \sqrt{2M_1T_1}\sqrt{2M_4T_4}\cos\theta_4 \quad . \tag{11}$$

It is possible to define three parameter numerically exactly known,

$$a = \frac{M_3 + M_4}{M_3 - M_1} \quad , \quad b = \frac{M_3 Q}{M_3 - M_1} \quad , \quad g = \frac{\sqrt{M_1 M_4}}{M_3 - M_1}$$

by meaning that the knowledge of their values is affected by a negligible error in comparison with the experimental indetermination on both the energy and the scattering angle of the α particle. Eq. (11) can then be written as

$$T_1 + (b - aT_4) = -2g\sqrt{T_1}\sqrt{T_4} \cdot \cos\theta_4 \tag{12}$$

and solved with respect to T_1 as an ordinary 2^{nd} degree equation. With simple algebraic manipulations, the analytical solution for the neutron energy as a function of the detected α particle parameters is

$$T_1(T_4, \theta_4) = (a + 2g^2\cos^2\theta_4)T_4 - b + 2g \cdot \cos\theta_4 \sqrt{(a + g^2\cos^2\theta_4)T_4^2 - bT_4} \tag{13}$$

which has to fulfill the constraint imposed by the reality of the square root. This condition is summarized by the request

$$T_4 \cdot \left[(a + g^2\cos^2\theta_4)T_4 - b\right] \geq 0 \tag{14}$$

but, as T_4 represents the neutron energy which is certainly positive, Eq. (14) becomes a lower limit to the energy of the outcoming ${}^4_2He$ particle,

$$T_4 \geq \frac{b}{a + g^2\cos^2\theta_4} \geq \left(1 + \frac{M_4}{M_3 - M_1}\right)^{-1} Q \quad . \tag{15}$$

The last value has been obtained with the choice $\cos\theta_4 = 1$ which is the maximum possible value of the cosine and refers to forward scattering ($\theta_4 = 0$). The pre–Q value is then the minimum fraction of the α particle energy in Q units which can be found in the detection process, i.e.

$$T_4 \geq 1.589\ MeV$$

and lies below the D–D typical fusion energy (2.547 MeV).

3. Error estimates

Errors on the neutron energy T_1 are evaluated according to the canonical errors propagation theory with the hypothesis of linear independent errors on θ_4 and T_4,

$$\Delta T_1 = \sqrt{\left(\frac{\partial T_1}{\partial \theta_4}\right)^2 (\Delta\theta_4)^2 + \left(\frac{\partial T_1}{\partial T_4}\right)^2 (\Delta T_4)^2} \tag{16}$$

The derivatives of T_1 with respect to T_4 and θ_4 can be analytically evaluated directly from Eq. (13),

$$\frac{\partial T_1}{\partial T_4} = a + 2g^2\cos^2\theta_4 + 2g\cdot\cos\theta_4 \cdot \frac{2(a+g^2\cos^2\theta_4)T_4 - b}{\sqrt{(a+g^2\cos^2\theta_4)T_4^2 - bT_4}} \tag{17}$$

$$\frac{\partial T_1}{\partial \theta_4} = -2gT_4\cdot\sin\ \theta_4 \cdot \left[2g\cdot\cos\theta_4 + \frac{(a+3g^2\cos^2\theta_4)T_4 - b}{\sqrt{(a+g^2\cos^2\theta_4)T_4^2 - bT_4}}\right] \tag{18}$$

while the errors ΔT_4 and $\Delta\theta_4$ which affect the measured values of the α particle scattering energy and angle can be related to the sensitivity of the detector [8].

It can be deduced that the constraint (15) must be fulfilled strictly ($T_4 > 1.589\ MeV$) in order to avoid singularities in the denominators of (17) and (18).

In what follows only the $\theta_4 = 0^o \div 90^o$ angular range has been considered as this corresponds to α particles scattered in the forward direction and it is the most interesting interval of θ_4 in the detection process (see Fig. 1). Attention has been focused on α particles generated by neutrons coming from D–D and D–T nuclear reactions and $\frac{\pi}{4}$ angle has been chosen to illustrate the behaviour of the errors evaluated according to Eq. (16).

Results and discussion

A phenomenological approach based on energy–momentum conservation rule has been used to study $Li(n,\alpha)T$ nuclear process involved in the neutron detection procedure oriented to plasma diagnostics [10].

The expected values of the α particles produced by neutrons whose energies are exactly the D–D ($B_{D-D} = 2.475\ MeV$) and D–T ($B_{D-T} = 14.076\ MeV$) peaks fusion energies are listed in Tab. I and sketched in Fig. 2 as a function of the scattering angle measured in the laboratory frame. The lower limit given by Eq. (15) has also been reported on the plot.

Numerical values of the calculated error bars are listed in Tab. II and Tab. III for the two cases of D–D and D–T originated neutrons respectively. A fixed scattering angle ($\theta_4 = 45^o$) has been chosen in order to lower the number of variables involved in the computation. The monotonic behaviour of these errors as functions of α particle energy and angle uncertainties is rather evident but the dependence on the α energy uncertainty is clearly stronger, while the dependence on the angular resolution is rather weak. In particular an energy resolution of the α particle detector well below 0.2 % and 0.4 % seems to be requested in the two cases respectively.

Error percentages have been chosen according to the following double list of values:

$$\Delta E_\alpha\% : 0 \ , 0.2 \ , 0.4 \ , 0.6 \ , 0.8 \ , 1.0$$

$$\Delta\theta_4\% : 0 \ , 0.01 \ , 0.05 \ , 0.1 \ , 0.5 \ , 1.0$$

The surface plots reported in Figs. 3 and 4 show the behaviour of the errors ΔE_n at fixed 45^o scattering angle and for the two different cases of neutrons originated by D–D and D–T fusion reactions respectively. The different dependence on angle and energy resolution is quite evident. The scattering angle of α particle is always 45^o. Figs. 5 and 6 display the dependence on the energy resolution in more detail and for particularly low values of the variable. It is clear that, for D–D reaction case, an energy resolution below 0.1 % is needed, while, for the case of D–T reaction, the requested resolution is more affordable. The FWHM of the neutron energy distribution is also shown for reference. It can be interpreted as the upper limit to the indetermination of the corresponding particle energy.

Finally the ΔE_n errors at fixed α particle energy and angle indetermination have been plotted vs. the scattering angle θ_4 as shown in Fig. 7. It is quite evident that at large angles, where the damage of the detector should be sensitively reduced, the errors on the neutron energy drop out due to the angular dependence of Eq. (16). The fixed values for α particle energy and angle errors are quoted here only for giving a reference. Obviously, the situation is more favourable for D–T case, where the drop in neutron energy error is much stronger.

Conclusions

In the hypothesis of using ^6Li target to monitor neutrons coming out from plasma D–D and D–T reactions, we have obtained in the present work the energy and angular resolution needed for the α particle detector, in order to suitably monitor the plasma temperature by the neutron energy spread around the peaks at 2.45 MeV and 14 MeV respectively.

What it turns out is that, while the constant angular resolution is rather weak, in order to fulfill the energy resolution request, a very precise and sophisticated α particle spectrometer should be available, with an energy resolution of the order of 0.1 %. It could well be that such a kind of spectrometer is outside of the present technical possibilities.

References

[1] G.F. Knoll - *Radiation detection and measurement* , 2^{nd} edition, John Wiley & sons, New York (1989)

[2] J.B. Marion and J.L. Fowler - *Fast Neutron Physics* - Part 1 & 2 - New York (1960)

[3] K.A. Verschuur - *Neutron transport calculations in support of neutron diagnostics at JET* , Netherlands Energy Research Foundation Report, ECN–86–097

[4] C. Manfredotti, A. Zanini, C. Ongaro and M. Boero - Exp. Phys. Dept. Int. Report (1991)

[5] R. Dierckx - *IGNITOR: particle diagnostics and physics R & D* ,working paper, EURATOM (Ispra), November 1988

[6] O.N. Jarvis, M.T. Swinhoe and P. Dixon - Proposed diagnostic systems for JET - 4^{th} ASTM-Euratom Symposium on Reactor Dosimetry, NBS - Washington, March 22-26, 1982

[7] E. Segré - *Nuclei and Particles* - 2^{nd} edition, W.A. Benjamin Inc., Berkeley (1977)

[8] J.C. Barton, C.J. Hatton, J.E. McMillan, Jour. of Phys. G17 (1991) 1885

[9] J. Kallne, P. Batistoni and G. Gorini, Rev. of Sci. Instr. 62 (1991) 2871

[10] F.L. Ribe, Rev. Mod. Phys. 47 (1975) 7

Table Captions

Tab. I - Expected energy values of the α particle as a function of the emission angle, for the cases of D–D and D–T fusion reactions.

Tab. II - Uncertainty in the neutron energy, expressed in MeV, as a function of angular resolution and energy resolution of the α particle detector, in the case of D–D reaction and for an α scattering angle of 45°.

Tab. III - Uncertainty in the neutron energy, expressed in MeV, as a function of angular resolution and energy resolution of the α particle detector, in the case of D–T reaction and for an α scattering angle of 45°.

Figure Captions

Fig. 1 - Kinematics of the $Li(n,\alpha)T$ scattering process in the laboratory frame.

Fig. 2 - Dependence of the α–particle energy on the emission angle for D–D and D–T reactions.

Fig. 3 - Surface plot of the uncertainty in the neutron energy, expressed in MeV, as a function of both the α particle energy and angle errors. The lines on the surface plot represent data reported in Tab. II. The θ_4 angle has been fixed at 45° while the neutron energy has been chosen as the E_n value of the D–D produced neutron.

Fig. 4 - Surface plot of the uncertainty in the neutron energy, expressed in MeV, as a function of both the α particle energy and angle errors. The lines on the surface plot represent data reported in Tab. III. The θ_4 angle has been fixed at 45° while the neutron energy has been chosen as the E_n value of the D–T produced neutron.

Fig. 5 - Uncertainty in the neutron energy, expressed in MeV, as a function of the error in α particle energy, for two cases of angular resolution (D–D reaction) and $\theta_4 = 45^o$

Fig. 6 - Uncertainty in the neutron energy, expressed in MeV, as a function of the error in α particle energy, for two cases of angular resolution (D–T reaction) and $\theta_4 = 45^o$

Fig. 7 - Behaviour of neutron energy uncertainty (MeV) as a function of the α–particle scattering angle, for fixed angular and energy resolutions and for D–D and D–T reactions respectively.

D-D and D-T originated α particles		
θ_4 [deg]	$E_\alpha^{(D-D)}$ [MeV]	$E_\alpha^{(D-T)}$ [MeV]
0^o	4.7042	14.1272
11.25^o	4.6570	13.9114
22.30^o	4.5198	13.2878
33.45^o	4.3045	12.3238
45.0^o	4.0291	11.1189
56.15^o	3.7153	9.7880
67.30^o	3.3850	8.4432
78.45^o	2.4746	7.1776
90.0^o	2.7510	6.0551

TAB. I

ΔE_α \ $\Delta\theta_4$		0 %	0.01 %	0.05 %	0.1 %	0.5 %	1.0 %
		0.0000	0.0045	0.0225	0.0450	0.2250	0.4500
0.0 %	0.000	0.000	0.001	0.004	0.009	0.044	0.088
0.2 %	0.004	0.068	0.068	0.068	0.069	0.081	0.111
0.4 %	0.007	0.137	0.137	0.137	0.137	0.147	0.162
0.6 %	0.011	0.205	0.205	0.205	0.205	0.210	0.223
0.8 %	0.015	0.273	0.273	0.273	0.273	0.277	0.287
1.0 %	0.019	0.342	0.342	0.342	0.342	0.344	0.353

TAB. II

ΔE_α \ $\Delta\theta_4$		0 %	0.01 %	0.05 %	0.1 %	0.5 %	1.0 %
		0.0000	0.0045	0.0225	0.0450	0.2250	0.4500
0.0 %	0.000	0.000	0.001	0.006	0.013	0.065	0.130
0.2 %	0.007	0.070	0.070	0.071	0.071	0.096	0.148
0.4 %	0.013	0.141	0.141	0.141	0.141	0.155	0.192
0.6 %	0.020	0.211	0.211	0.211	0.211	0.221	0.248
0.8 %	0.026	0.281	0.281	0.281	0.281	0.287	0.310
1.0 %	0.033	0.351	0.351	0.351	0.352	0.357	0.375

TAB. III

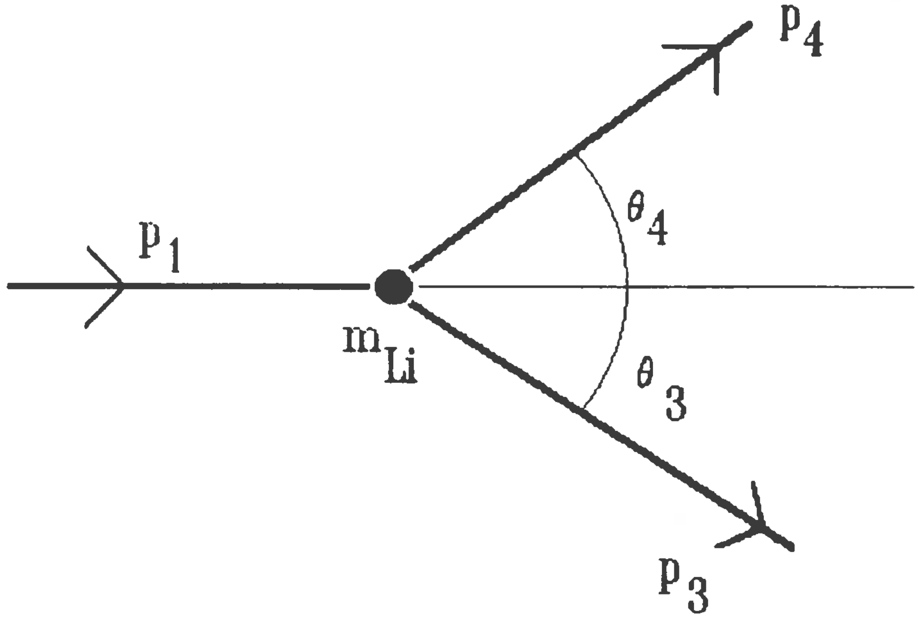
p_4
θ_4
p_1
m_{Li}
θ_3
p_3

FIG. 1

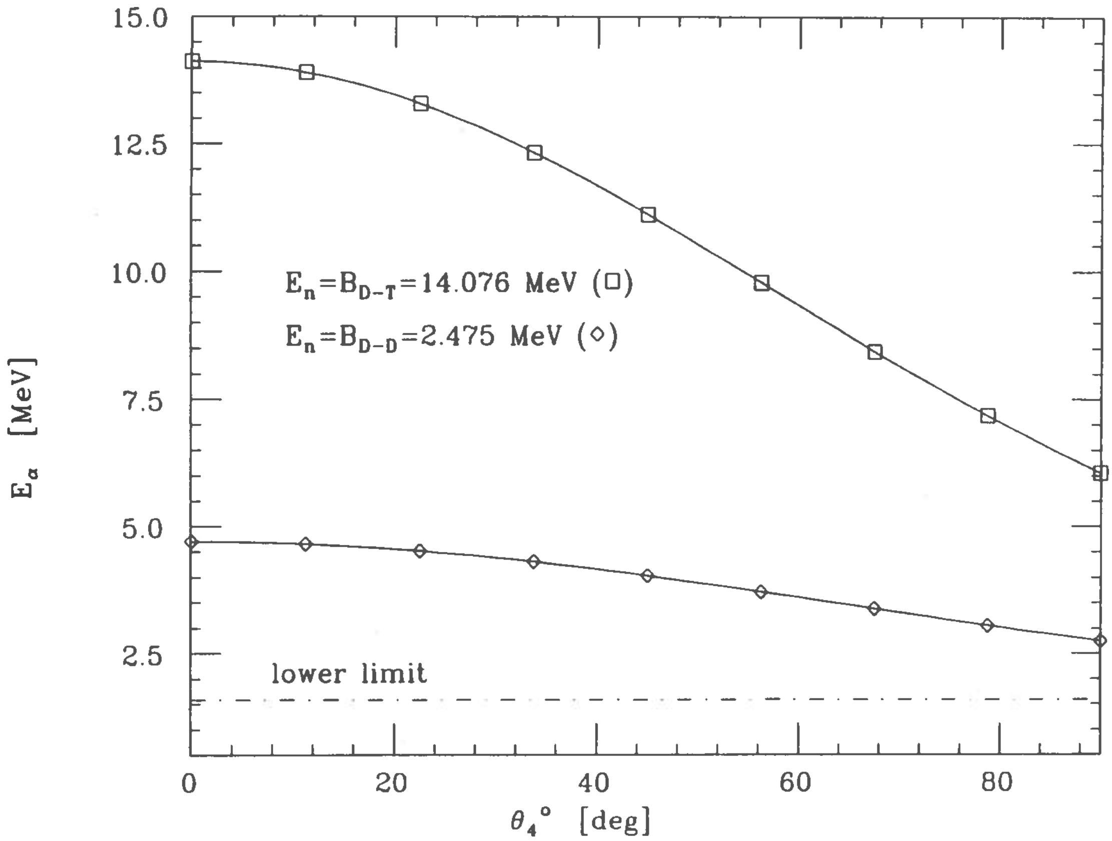
15.0
12.5
10.0
7.5
5.0
2.5
$E_n=B_{D-T}=14.076$ MeV (□)
$E_n=B_{D-D}=2.475$ MeV (◇)
E_α [MeV]
lower limit
0
20
40
60
80
$\theta_4°$ [deg]

FIG. 2

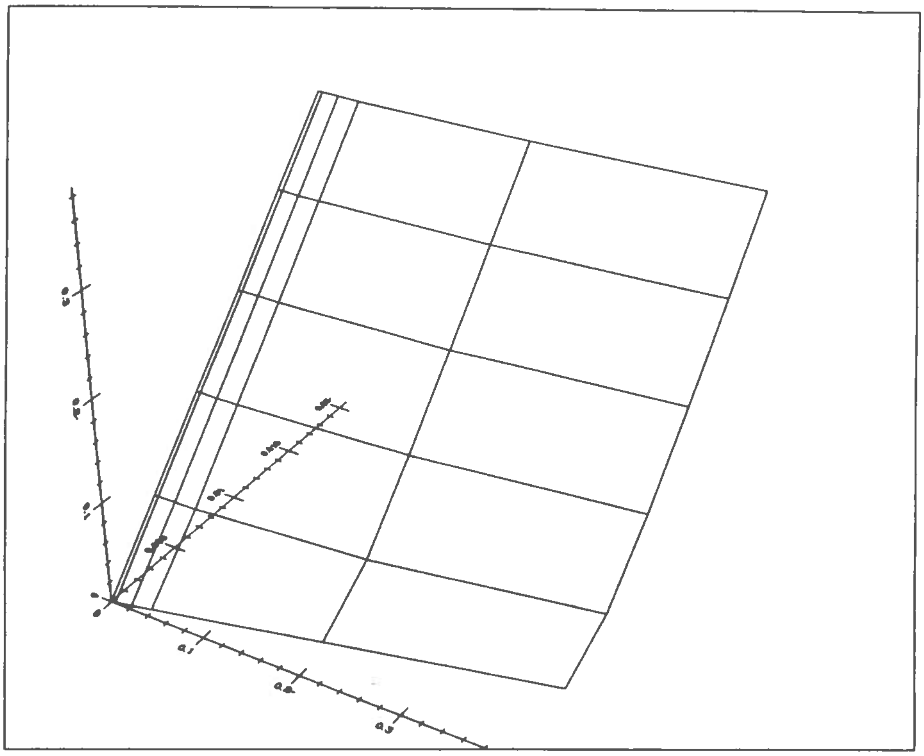

D−D θ_4=45° E_α=1.878 MeV

FIG. 3

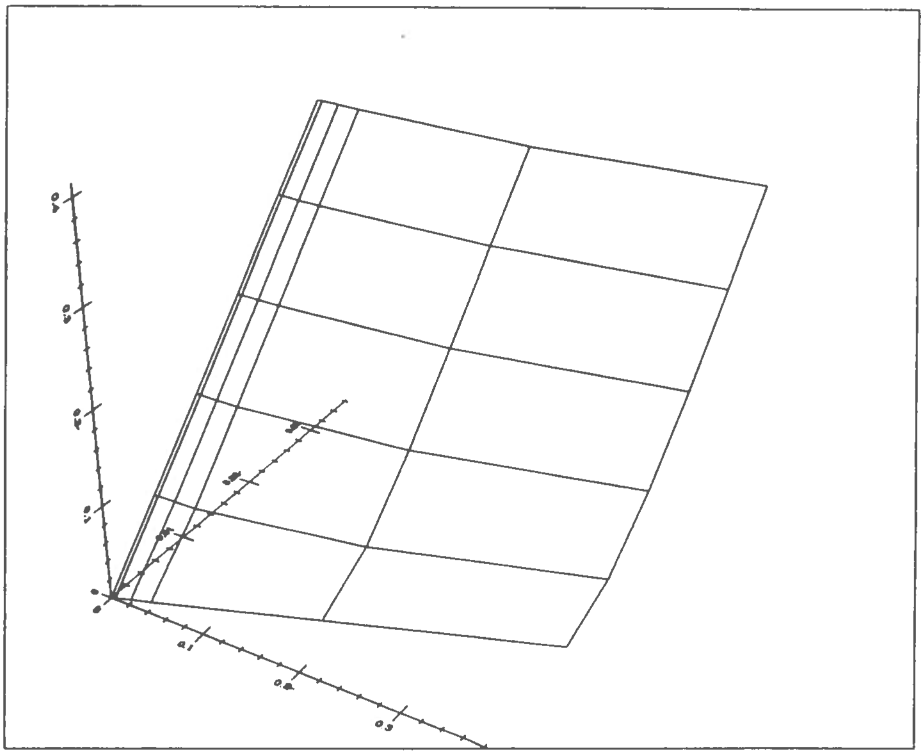

D−T θ_4=45° E_α=3.298 MeV

FIG. 4

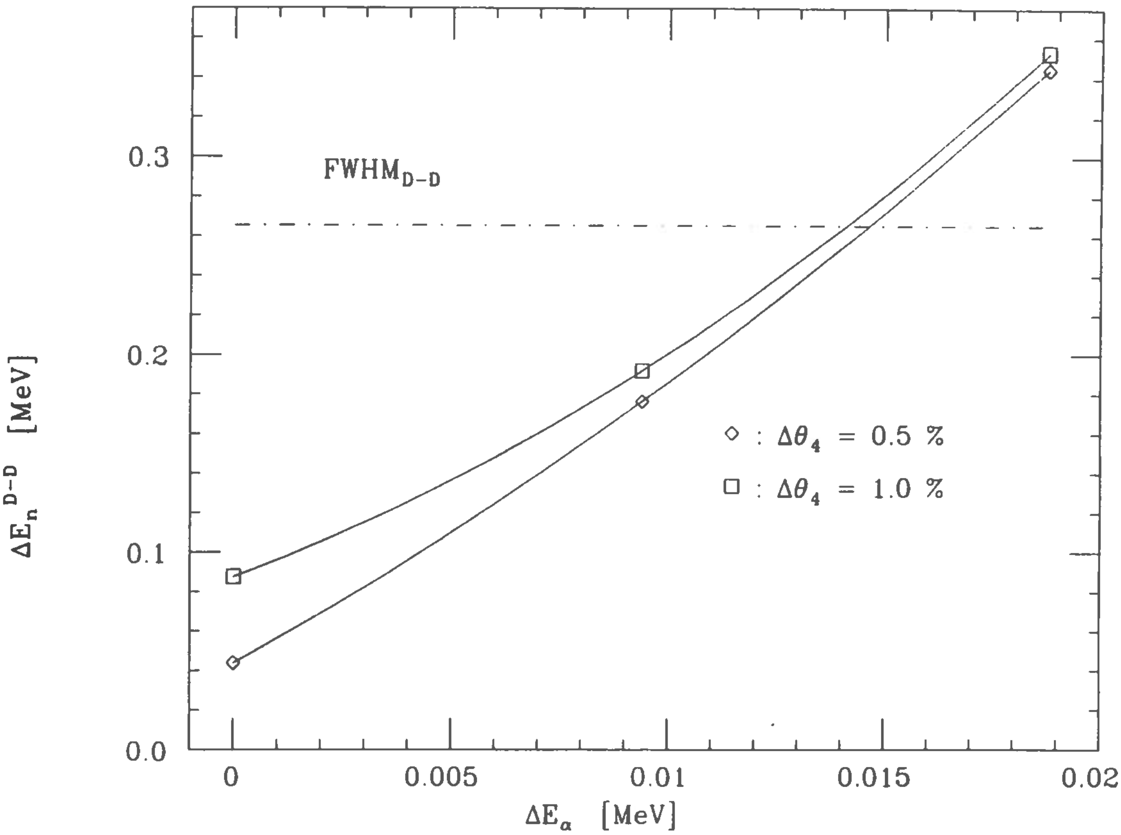

0.3
0.2
0.1
0.0
0
0.005
0.01
0.015
0.02
FWHM$_{D-D}$
ΔE_n^{D-D} [MeV]
ΔE_α [MeV]
◇ : $\Delta\theta_4$ = 0.5 %
□ : $\Delta\theta_4$ = 1.0 %

FIG. 5

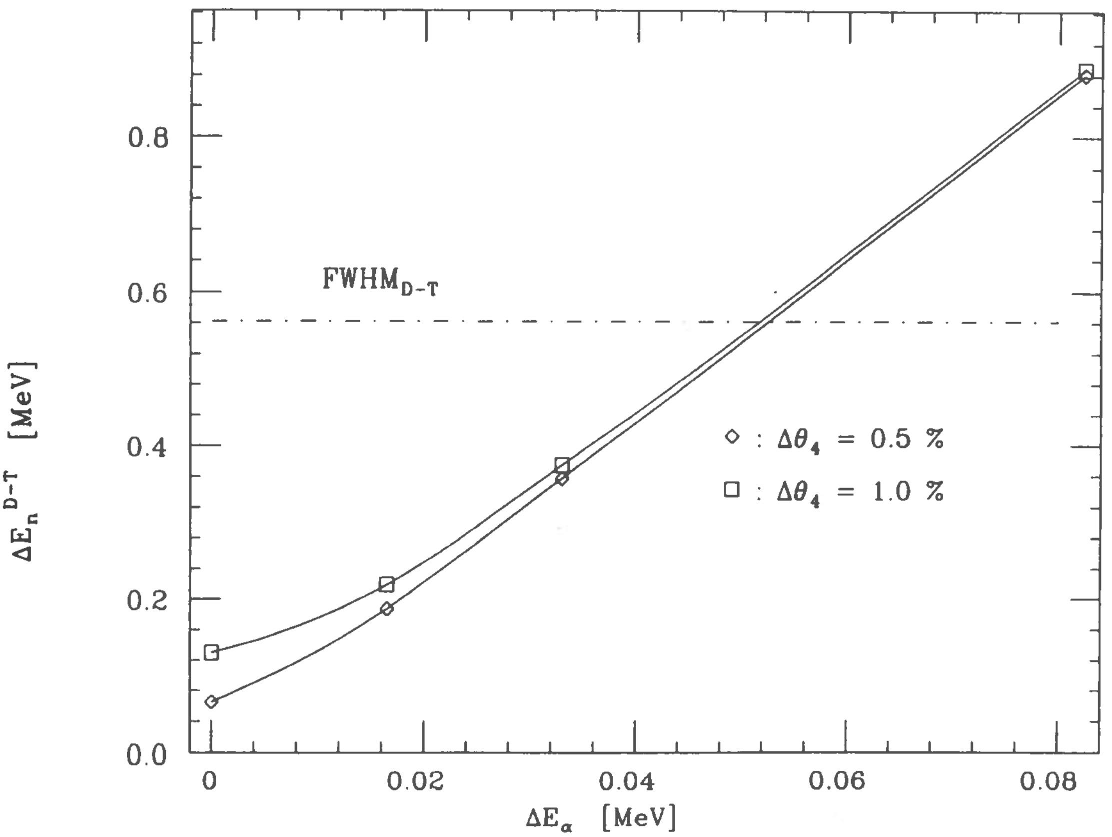

0.8
0.6
0.4
0.2
0.0
0
0.02
0.04
0.06
0.08
FWHM$_{D-T}$
ΔE_n^{D-T} [MeV]
ΔE_α [MeV]
◇ : $\Delta\theta_4$ = 0.5 %
□ : $\Delta\theta_4$ = 1.0 %

FIG. 6

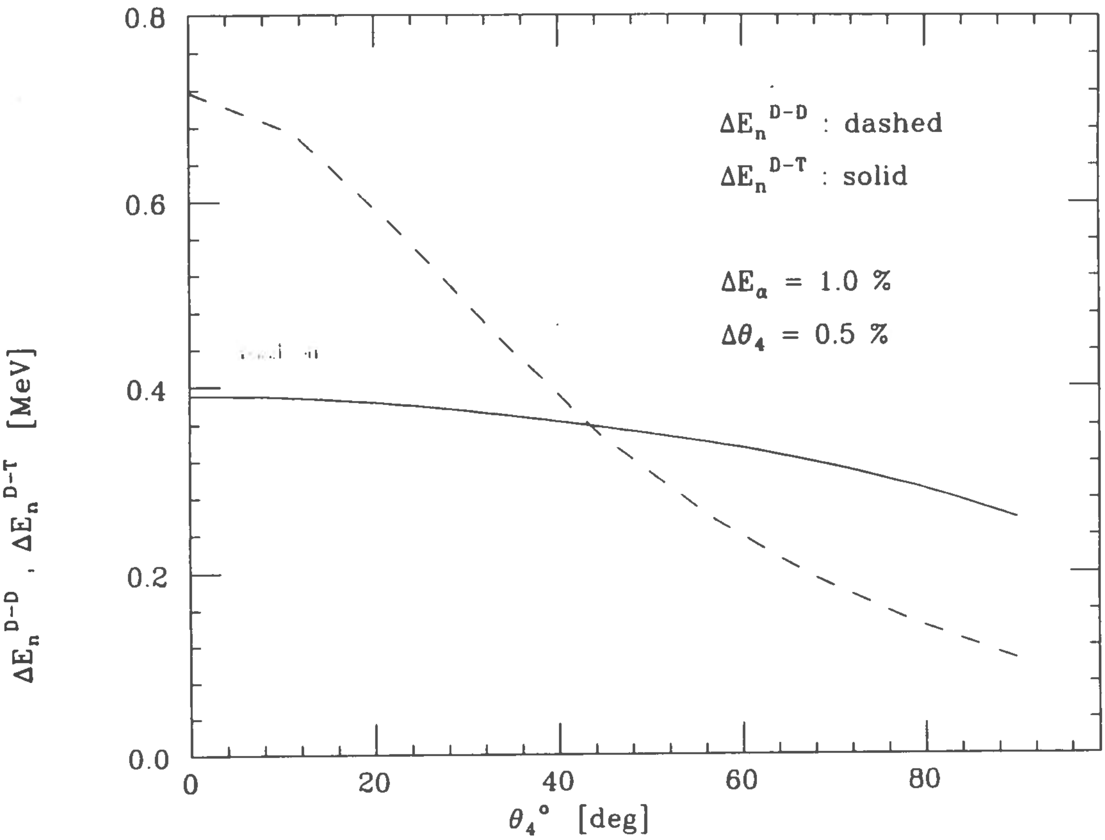

0.8
0.6
0.4
0.2
0.0
ΔE_n^{D-D} , ΔE_n^{D-T} [MeV]
ΔE_n^{D-D} : dashed
ΔE_n^{D-T} : solid
ΔE_α = 1.0 %
$\Delta\theta_4$ = 0.5 %
0
20
40
60
80
$\theta_4°$ [deg]

FIG. 7